Phase diagram of antimony up to 31 GPa and 835 K

The Phase Diagram of Antimony to 31 GPa and 835 K

A. L. Coleman, M. Stevenson, and M. I. McMahon

SUPA, School of Physics & Astronomy,

and Centre for Science at Extreme Conditions,

The University of Edinburgh, Edinburgh, EH9 3FD, UK

S. G. Macleod

Atomic Weapons Establishment, Aldermaston, Reading,

RG7 4PR, United Kingdom and Institute of Shock Physics,

Imperial College London, SW7 2AZ, United Kingdom

(Dated: March 5, 2018)

Abstract

X-ray powder diffraction experiments using resistively-heated diamond anvil cells have been conducted in order to establish the phase behaviour of antimony up to 31 GPa and 835 K. The dip in the melting curve at 5.7 GPa and 840 K is identified as the triple point between the Sb-I, incommensurate Sb-II and liquid phases. No evidence of the previously-reported simple cubic phase was observed. Determination of the phase boundary between Sb-II and Sb-III suggests the existence of a second triple point in the region of 13 GPa and 1200 K. The incommensurate composite structure of Sb-II was found to remain ordered to the highest temperatures studies – no evidence of disordering of the guest-atom chains was observed. Indeed, the modulation reflections that arise from interactions between the host and guest subsystems were found to be present to the highest temperatures, suggesting such interactions remain relatively strong in Sb even in the presence of increased thermal motion. Finally, we show that the incommensurately modulated structure recently reported as giving an improved fit to diffraction data from incommensurate Ba-IV can be rejected as the structure of Sb-II using a simple density argument.

PACS numbers: 61.50.Ks,62.50.–p

I. INTRODUCTION

Antimony is one of the few elemental metals or semimetals that does not crystallise into a cubic or hexagonal close-packed structure at ambient conditions[1]. Instead, it forms the rhombohedral A7 structure (Sb-I), with space group $R\bar{3}m$, which is a Peierls-distorted simple-cubic (sc) structure. Under static compression at room temperature there have been various reports of a transition from the A7 structure to the undistorted sc structure. Initially this was reported to be a continuous transition occurring at 7 GPa[2], but with the improvement of x-ray diffraction techniques, the same group later reported that the transition was in fact first order[3]. However, the single-crystal study of Schiferl[4] and the later, high-resolution powder diffraction study of Degtrayeva *et al.*[5] showed that while the A7 structure approaches the sc structure on compression up to 8 GPa, the latter is never obtained. Rather, there is a first-order transition at that pressure to a tetragonal incommensurate composite structure (Sb-II)[6–8] which is stable up to 28.8 GPa (at 300 K) where it transforms to the body-centred cubic (bcc) Sb-III phase[5,9].

The incommensurate composite structure is an unusually complex structural form, observed first in barium[10] and subsequently in a selection of elements from Groups 1, 2, 3

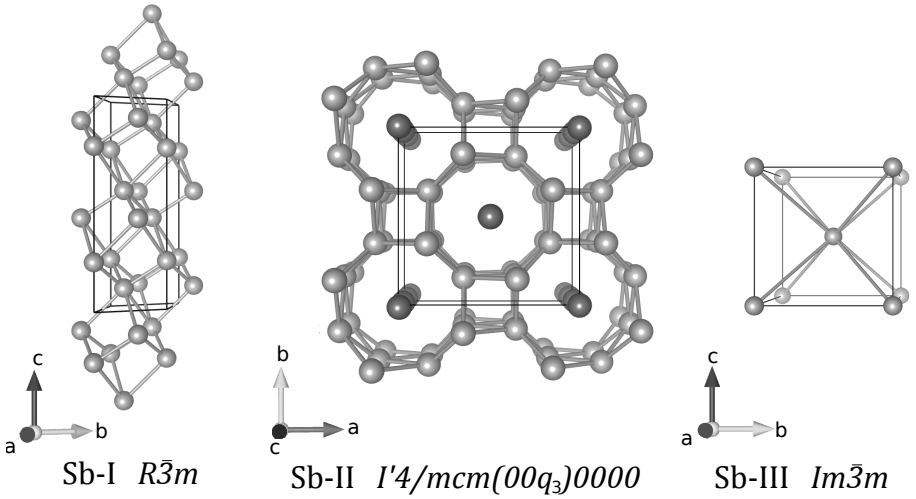

FIG. 1. The crystal structures (not to scale) of Sb-I, Sb-II and Sb-III. In Sb-I, bonds are shown between the atoms to highlight the distorted simple cubic nature of the structure. In the host-guest structure of Sb-II, the host subsystem is shown in light grey, and the chains of guest atoms are shown in dark grey.

and 15[11]. The Sb-II composite structure comprises an 8-atom body-centred tetragonal host subsystem (space group $I4/mcm$) with channels running along the c-axis. Within these channels run linear chains of guest atoms, which form a 2-atom body-centred tetragonal guest subsystem (space group $I4/mmm$) which is incommensurate with the host along their common c axis. The same composite structure is observed in Bi between 2.8 and 7.7 GPa at 300 K[12]. It is advantageous to describe the composite structure of Sb-II in four dimensional (4D) superspace, where its superspace group is $I'4/mcm(00q_3)0000$, with $q_3 = c_H/c_G$, and

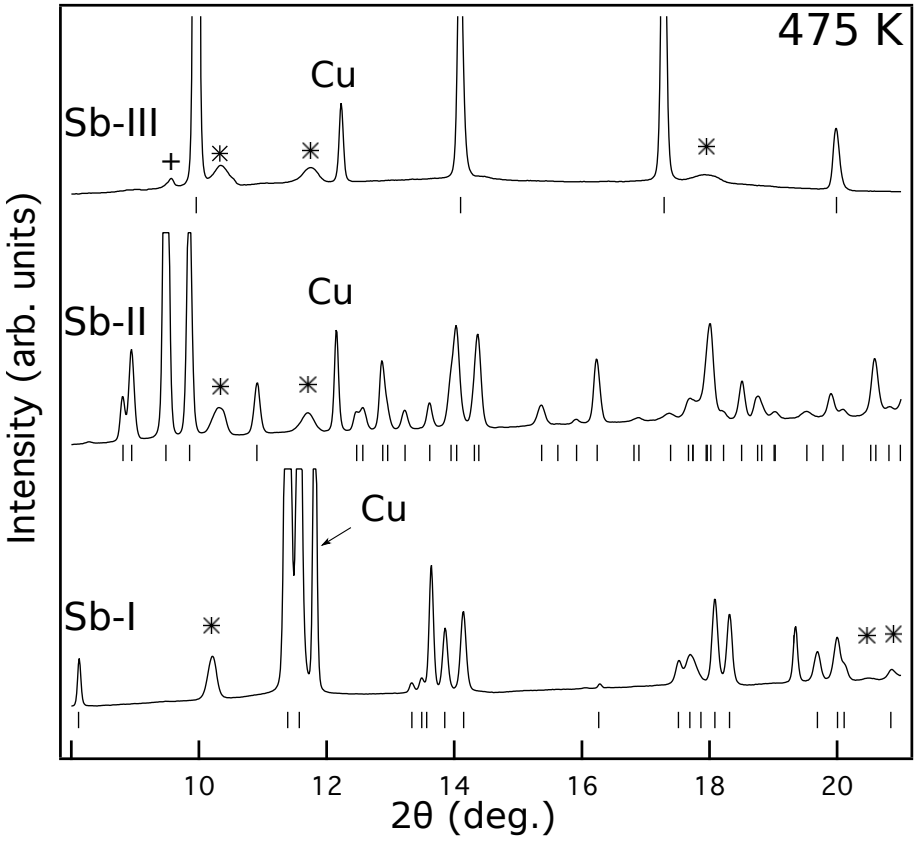

FIG. 2. Waterfall plot illustrating the diffraction patterns obtained from the three distinct phases identified during the experiment: the rhombohedral A7 phase (Sb-I), the incommensurate composite phase (Sb-II), and the bcc phase (Sb-III). The data shown were collected on an isotherm at ∼475 K, at pressures of 6.2, 23.1 and 27.6 GPa, respectively. Peaks from the rhenium gasket are marked with asterisks and the copper pressure calibrant peaks are labeled as such. The weak peak marked with a + in the profile from Sb-III is the remnant of the the intense (2110) reflection from Sb-II that remains after the onset of the transition to Sb-III. The most intense peaks from all three phases have been cropped for clarity.

c_H and c_G are the c-axis repeat distances of the basic host and guest structures, respectively. In superspace, the diffraction peaks are indexed using four integers $(hklm)$, where reflections from the host subsystem of the basic composite structure have indices $(hkl0)$, those from the guest subsystem have indices $(hk0m)$, and the $(hk00)$ reflections are common to both host and guest. Interactions between the host and guest subsystems can result in shifts with respect to the lattice periodic atomic positions, described by modulation functions within the superspace formalism, giving rise to additional weak modulation reflections $(hklm)$ with both $l \neq 0$ and $m \neq 0$. Such modulation reflections are observed in powder diffraction patterns from Sb-II at 300 K[7,12,13], and indeed are more intense in Sb-II than in the incommensurate composite structures of any other element. The total number of atoms in a unit cell of Sb-II is non-integer and is equal to $N = 8 + 2q_3$. Since the value of q_3 varies with pressure[7], N is pressure dependent.

Degyareva *et al.* reported an intraphase transition from Sb-II to another composite structure (Sb-IV) comprising body-centred monoclinic host and guest subsystems[7]. Sb-IV, with superspace group $I'2/c(q_1 0 q_3)00$, is observed only between 8.2 and 9.0 GPa on pressure increase and between 8.0 and 6.9 GPa on pressure decrease. The occurrence of an intraphase transition between two composite structures is not unique to antimony and has also been observed in barium[10] and strontium[14]. Another phenomenon observed in composite structures is the loss of long range order in the chains of guest atoms, resulting in the disappearance of the $(hk0m)$ and $(hklm)$ ($l \neq 0$ and $m \neq 0$) Bragg peaks. This "chain-melting" was first observed in rubidium[15,16], subsequently in potassium[17], and, more recently, it has been observed in dynamically-compressed scandium at higher temperatures[18]. There have been relatively few high-temperature, high-pressure studies of Sb, although the melt curve has been determined up to $\sim$ 6.5 GPa, with a triple point reported near 5.7 GPa and $\sim$ 840 K[19]. It is not known, therefore, whether the incommensurate composite structure of Sb is still the stable phase under such conditions, and, if so, whether it undergoes a chain-melting transition at high temperatures even though the intensity of the $(hklm)$ modulation reflections at 300 K suggests relatively strong interactions between the host and guest subsystems.

Here we report high-pressure high-temperature studies of Sb to 31 GPa and 835 K, using resistively heated diamond anvil cells. Over this P-T range we observed only the Sb-I, Sb-II and Sb-III phases, and saw no evidence of either Sb-IV, or the simple cubic

phase. Furthermore, we observe no evidence of any chain melting up to 835 K. Indeed, the ($hklm$) modulation reflections arising from the interactions between the host and guest subsystems were very clearly observed to the highest temperatures, suggesting that such interactions remain strong in Sb even at elevated temperatures. We also show that the alternative structural model recently reported for the structure of Ba-IVb can be rejected as the structure of Sb-II using a simple density argument.

II. EXPERIMENTAL DETAILS

Powder diffraction data were collected on beamline I15 at the Diamond Light Source, using an X-ray beam with a diameter of 20 μm and a wavelength of 0.4246 Å. Resistively-heated, gas-membrane driven diamond anvil cells (DACs)[20], contained within a custom-designed vacuum vessel, and capable of heating to above 800 K[21], were utilised to collect data on Sb up to 835 K and a maximum pressure of 31 GPa. The high-purity polycrystalline Sb sample used in this experiment was obtained from Lawrence Livermore National Laboratory as a $\sim$8 μm thick deposited layer, and small pieces were loaded into the cell along with a small piece of 5 μm thick copper foil which was used for pressure calibration. A small amount of mineral oil was used as a pressure transmitting medium and rhenium was used as the gasket material with a sample chamber diameter of 80 μm. The sample pressure was obtained from the thermal equation of state (EoS) of copper published recently by Sokolova *et al.*[22]. In one DAC a partial reaction was observed between the Sb sample and the copper pressure calibrant to form Cu_2Sb. This reaction occurred only in the DAC used to collect data at $\sim$650 K, and arose because the copper was loaded into this cell such that it was in direct contact with the Sb sample. Four separate data collections were conducted, comprising isothermal compressions at approximately 300, 475, 650 and 720 K. Data were collected only on pressure increase, and the sample temperature was measured using a K-type thermocouple which was attached to one of the diamond anvils, close to the sample. The diffraction data were collected using a Mar345 image-plate detector which was placed approximately 385 mm from the sample. The 2D diffraction images were integrated using the FIT2D software[23] and the resulting 1D profiles were analysed using both the JANA2006 software system[24] and individual peak fitting followed by least-squares analysis of d-spacings. Analysis of the effects of non-hydrostaticity on the sample were analysed using Multifit[25].

III. RESULTS AND DISCUSSION

Figure 2 shows a series of diffraction patterns collected on pressure increase at ∼475 K. At this temperature we observed the Sb-I → Sb-II transition at 7.1(1) GPa, and the Sb-II → Sb-III transition at 25.1(5) GPa. We saw no evidence of the monoclinic Sb-IV composite phase. Tickmarks beneath the profiles in Figure 2 show the calculated locations of the Bragg peaks from each of the three phases, while those peaks identified with asterisks arise from scattering from the rhenium gasket. The quality of the diffraction patterns is excellent, although the relative intensities of the peaks in Sb-I were strongly affected by preferred orientation, arising from the deposited nature of the Sb sample.

We observed no evidence of the simple cubic phase of Sb on pressure increase at any temperature, in agreement with the earlier high-temperature study of Iwasaki and Kikegawa to 11.5 GPa and ∼ 600 K[26]. Figure 3 shows the c/a ratio of Sb-I along each approximate

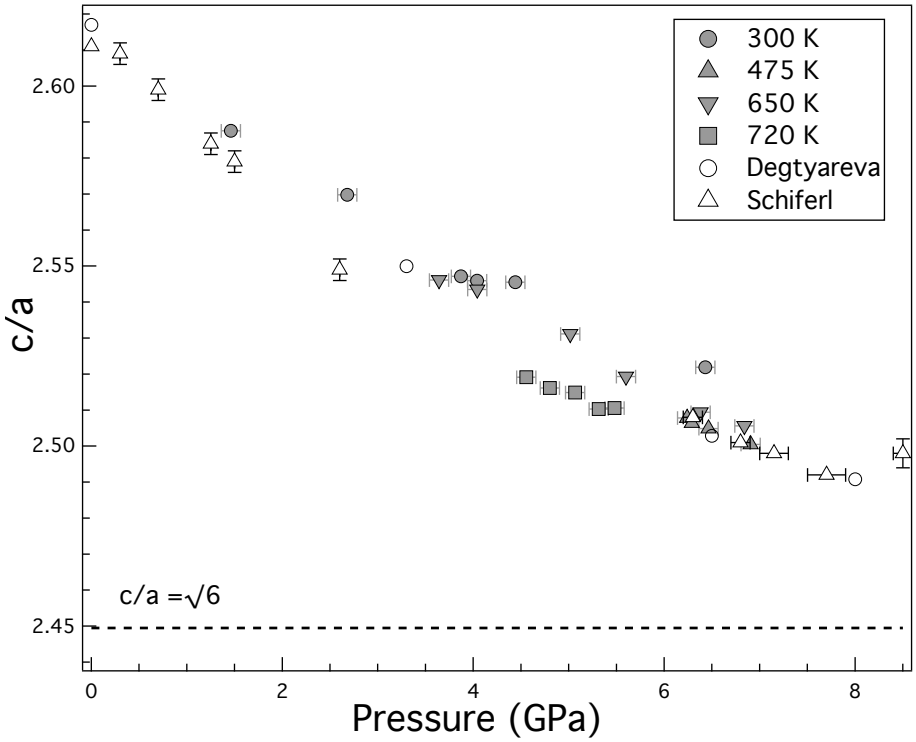

FIG. 3. The c/a ratio of Sb-I versus pressure, as obtained at different temperatures. Circles, upward pointing triangles, downward pointing triangles and squares show the present results obtained on compression at ∼293, ∼475, ∼650 and ∼720 K, respectively. Data from previous work by Schiferl[4] and Degtyareva[5] at room temperature are shown by unfilled triangles and circles, respectively.

isotherm, along with the previously-published room temperature data of Degtyareva *et al*[5] and Schiferl[4]. While the c/a ratio approaches the value of $\sqrt{6}$ required for the transition to the simple cubic phase, that value is never reached at any temperature prior to the transition to Sb-II. Our results suggest that the c/a ratio at the transition to Sb-II does decrease slightly with increasing temperature, but linear extrapolation suggests that the simple cubic phase will not be observed prior to the sample melting at ∼840 K.

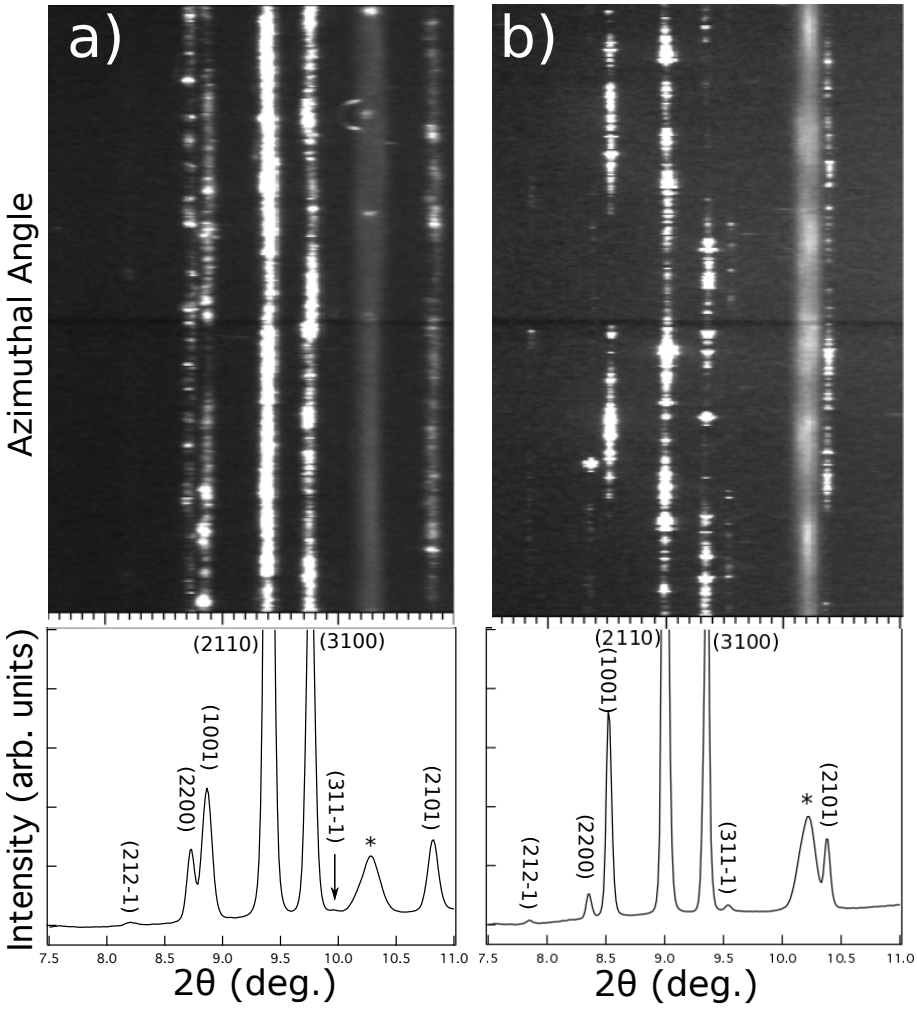

FIG. 4. 2D diffraction images and integrated profiles obtained from Sb-II at a) 19.4 GPa and 475 K, and b) 6.2 GPa and 720 K. The 2D images are plotted as 2θ–azimuthal-angle plots, such that Debye-Scherrer rings of constant radii appear as vertical lines. Peaks from the rhenium gasket are marked with asterisks. Recrystallisation of the sample results in increased visibility of the $(212\bar{1})$ and the $(311\bar{1})$ modulation peaks at higher temperatures in both the 2D images, and in the integrated profiles.

The diffraction profiles obtained from Sb-II, at all pressures and temperatures, contained ($hk0m$) diffraction peaks from the guest sub-structure, showing that the guest chains remain ordered to the highest temperatures studied here. This is in contrast to previous results on the composite structures of Rb, K and Sc, where the chains were found to become fully disordered, and the composite structure of Na at 147 GPa, where the chains were found to be partially disordered at 300 K[27]. The quality of the diffraction patterns from Sb-II also meant that it was possible to observe the weak ($hklm$) modulation reflections that arise from the interactions between the host and guest subsystems. While these peaks are stronger in Sb-II than in the composite structures of any other element, peak overlap in the powder diffraction profiles means that too few are visible to determine the P-T dependence of the structural modulations, which would require single-crystal diffraction data[12]. However, the relatively intense ($212\bar{1}$) and the ($311\bar{1}$) modulation peaks were observed both at room temperature, in agreement with our previous powder-diffraction study[5], and also to the highest P-T conditions studied (see, for example, Figure 4). Indeed, the ($311\bar{1}$) modulation reflection became sharper and *more* intense at higher temperatures. However, we believe these changes arose because of the re-crystallisation of the Sb sample at high temperatures, which gave rise to intense spots on the Debeye-Scherrer rings (see Figure 4), rather than from increased structural modulations. However, it is clear that significant host-guest interactions are still present in Sb-II well above room temperature, suggesting that any disordering of the guest chains, if it occurs, will only take place at considerably higher temperatures than have been studied here.

In treating the guest subsystem of Sb-II as a series of one-dimensional chains, it is possible to determine their effective Debye temperature, as we have done previously for the composite structure of Rb-IV[16]. For Sb-II, we estimate Θ_D=$\sim$540 K, considerably greater than the value of $\sim$178 K estimated for Rb-IV[16], and the value of 215 K obtained by Spal *et al.* for $Hg_{3-x}AsF_6$ at room temperature and ambient pressure[28]. While Θ_D is greater in Sb-II than in the chain-melted phases of Rb-IV and $Hg_{3-x}AsF_6$, it is difficult to correlate this directly with the melting temperature of the guest chains, which occurs as a consequence of the loss of correlation between the chains rather than being a one-dimensional melting process within each chain.

The sample recrystallisation observed above room temperature also reduced the effects of non-hydrostatic pressures on the diffraction profiles. In the data collected at room tem-

perature, small azimuthal variations in the radii of the Debye-Scherrer (D-S) rings were clearly visible in the 2D diffraction patterns collected from Sb-II between 9.3 and 28.6 GPa, but were negligible in the diffraction patterns obtained from Sb-I and Sb-III at the same temperature. While Sb-I is observed at lower pressures than Sb-II, where non-hydrostatic effects would be expected to be smaller, the absence of such effects in Sb-III, above 28 GPa, suggests that they were relieved at the Sb-II $\rightarrow$ Sb-III transition. Analysis of the 2D images collected above room temperature again showed no azimuthal variations in radii in D-S rings of the Sb-I and Sb-III phases, and while variations in the radii in D-S rings from Sb-II were found to persist at high temperatures, they were much less pronounced than at room temperature.

The proposed phase diagram of Sb to 31 GPa is shown in Figure 5. The phase boundaries, which were constructed such that they passed as closely as possible to the data points which marked the first appearance of a new phase, are completely consistent with the room temperature phase transition pressures reported by Degtyareva and Schiferl[4,5] although, as previously stated, the monoclinic Sb-IV phase is not observed in the current study. This is likely due to a gap in the coverage of the current data, as Sb-IV is stable over a very small pressure range on P increase, as discussed previously.

Our proposed phase boundary between Sb-I and Sb-II is in excellent agreement with that proposed by Khvostantsev and Siderov[29], and also agrees very well with the minimum in the melt curve previously observed at 5.7 GPa[19]. This minimum is thus confirmed as the triple point between the Sb-I, Sb-II, and liquid phases. The phase boundary between Sb-II and Sb-III is determined for the first time above room temperature, and is found to also have a negative slope. Extrapolation of the known melting curve to 6.5 GPa and the newly-determined Sb-II/Sb-III phase boundary suggests that there will be a second triple point between the liquid, Sb-II and Sb-III phases near 13 GPa and 1200 K (see Figure 5), although the exact location will depend on the curvature of the melting curve above 7 GPa. Further data will be required to locate its exact position.

Throughout this paper, we have analysed the data from Sb-II under the assumption that it has the incommensurate composite structure first proposed by McMahon *et al.* in 2000[5,6], and subsequently confirmed by Schwarz[13]. In a recent publication, Arakcheeva *et al.* have proposed an alternative interpretation of incommensurate host-guest structures, detailing the influence of a density wave within the channels of the incommensurate Ba-IVb

structure[30]. While this proposed structure for Ba-IVb is still incommensurate, it has an incommensurately modulated (referred to as "IM" in Ref[30]) rather than an incommensurate composite ("COMP" in Ref[30]) structure[8,31]. Arakcheeva *et al.* reported that the IM structure gave a better fit to their single-crystal diffraction data from Ba-IVb than the COMP structure, and warned that determining whether the IM or COMP structural models best fitted other data would require refinements with the highest quality data.

However, there is an alternative and simpler method of determining which of the two structural models fits best, as they calculate different sample densities from the same diffraction data. In the COMP model there are $8+2q_3$ Sb atoms in a unit cell of volume $a_H \times a_H \times c_H$,

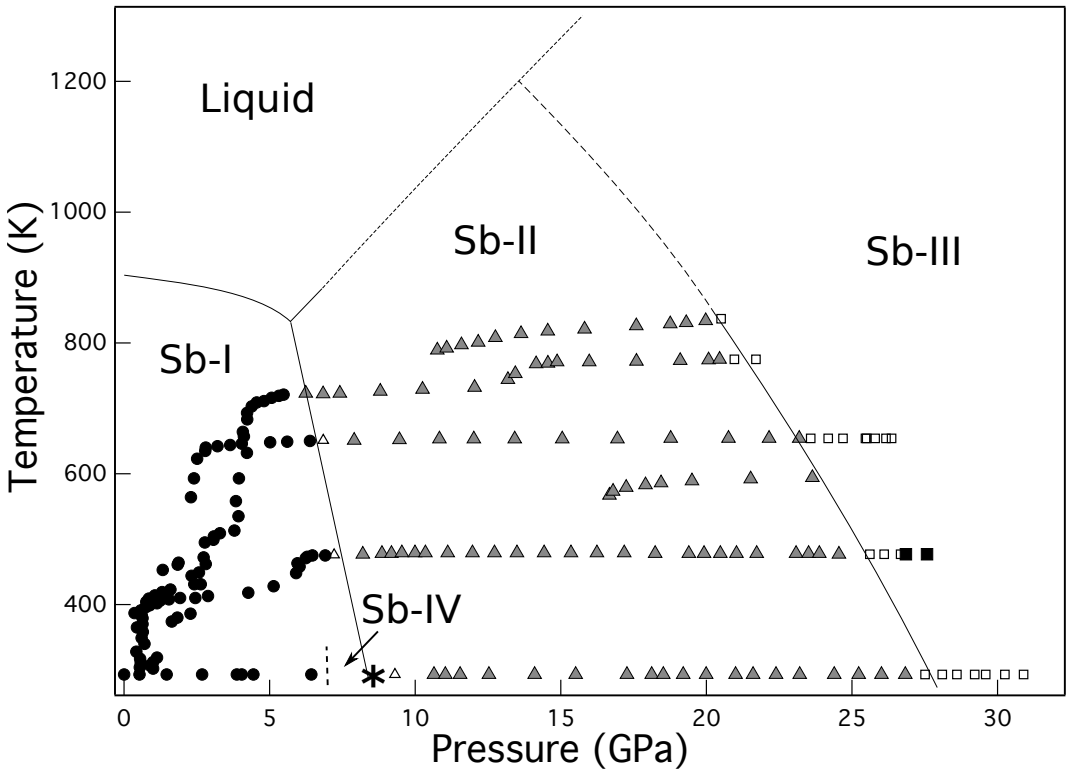

FIG. 5. The phase diagram of Sb to 31 GPa and 835 K. Circles, triangles and squares show the P-T conditions under which the Sb-I, Sb-II and Sb-III phases, respectively, were observed. Filled symbols indicate which single-phase profiles were observed, while unfilled symbols show where mixed phase profiles were obtained. The star symbol at 8.6 GPa and 300 K shows the location of the Sb-I $\rightarrow$ Sb-II transition reported by Degtyareva and Schiferl[4,5] and the Sb-IV phase, as reported by Degtyareva[5], is indicated by a dashed line at room temperature. The dashed melt curve is an extrapolation of the solid melt curve reported by Klement[19].

while in the IM model, assuming the same structure proposed for Ba-IVb, there are 20 Sb atoms in a unit cell of volume $\sqrt{2}a_H \times \sqrt{2}a_H \times c_H$. As a result, assuming a value of ∼1.31 for q_3 in Sb-II[5], the IM structure calculates a density for Sb-II that is ∼6% *less* than that calculated assuming the COMP structure, using the same diffraction pattern in each case.

Fortunately, the density of Sb-I and Sb-II have been measured directly to 9.8 GPa by Bridgman[32], using the piston displacement method, and these absolute measurements are

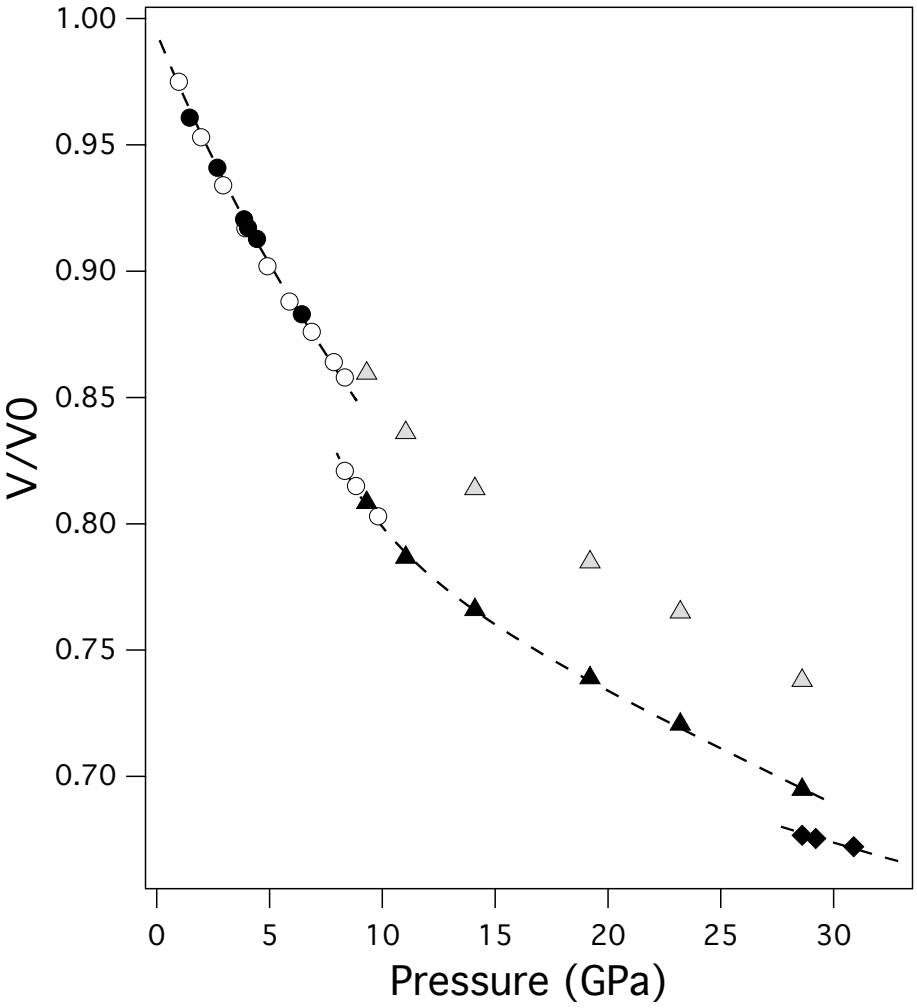

FIG. 6. The compressibility of Sb to 31 GPa at room temperature. Data points from Sb-I, Sb-II (analysed as an incommensurate composite (COMP) structure) and Sb-III are shown by filled circles, triangles and diamonds, respectively. The grey triangles show the volume of the Sb-II phase as calculated using the incommensurately modulated (IM) structure containing 20 atoms/cell described by Arakcheeva[30]. The data plotted with unfilled symbols are absolute volume measurements of Bridgman, made without phase determination[32].

shown in Figure 6. Also shown are the densities of Sb-II determined from the present room temperature diffraction data assuming both IM and COMP structural models. It is clear that the density calculated for Sb-II using the COMP structure is in excellent agreement with the data of Bridgman, as we noted previously[6], while the IM structure underestimates the density of Sb-II by ∼5%. Indeed, the IM structural model calculates an unphysical *decrease* in the density of Sb at the Sb-I → Sb-II transition, rather than the 3.7% *increase* in density reported by Bridgman[32].

Finally, the absence of the simple cubic phase in this study, and indeed in all recent high-pressure studies of Sb, led us to wonder whether its presence in the earlier studies of Vereschchagin, Kolobyanina and Kabalkina[2,3,33] arose because of the effects of non-hydrostaticity in these studies. To investigate this further we conducted some additional high-pressure high-temperature studies without the use of any pressure transmitting medium, with the gasket hole containing only Sb and the copper pressure marker. We again found no evidence of a transition to the simple cubic phase above room temperature – the c/a ratio of the rhombohedral A7 structure decreased with increasing pressure but did not reach $\sqrt{6}$ before the sample transformed to the incommensurate composite structure at ∼ 8 GPa.

IV. CONCLUSIONS

In conclusion, the high-pressure phase diagram of Sb has been determined to 31 GPa and 835 K using synchrotron x-ray diffraction and resistively-heated diamond anvil cells. The previously-reported minimum on the Sb melt curve at 5.7 GPa marks the triple point between the Sb-I, incommensurate Sb-II and liquid phases. The determination of the slope of the phase boundary between Sb-II and Sb-III suggests a second triple point near 13 GPa and 1200 K, although the exact location will depend on the curvature of the melting curve above 6.5 GPa. Further work is needed. Observation of the $(hk0m)$ diffraction peaks from the guest subsystem of Sb-II up to the highest temperatures reveals the guest chains to remain ordered, in contrast to the temperature-induced chain "melting" we have observed previously in Rb, K and Sc[15–18]. Indeed, the clear observation of the $(hklm)$ ($l \neq 0$ and $m \neq 0$) modulation peaks in the integrated profiles up to 835 K suggests that the structural modulations of the host and guest subsystems in Sb-II remain relatively unchanged on

heating, and therefore remain greater than those observed in other composite structures of the elements at room temperature. Given the greatly increased thermal motion of the guest-chains within the channels of the host framework at high temperatures, this is perhaps surprising.

V. ACKNOWLEDGEMENTS

British Crown Owned Copyright 2018/AWE. Published with permission of the Controller of Her Britannic Majestys Stationery Office. We thank Diamond Light Source (DLS) for provision of synchrotron time and support, and thank Dominik Daisenberger of DLS, Craig Wilson of AWE and Sarah Finnegan and Christian Storm of the University of Edinburgh for their help with the experiment.

---

[1] J. Donohue, *The Structures of the Elements*, A Wiley-interscience publication (John Wiley & Sons Incorporated, 1974).

[2] L. F. Vereschchagin and S. S. Kabalkina, Soviet Physics JETP **20**, 274 (1965).

[3] T. N. Kolobyanina, S. S. Kabalkina, L. F. Vereschangin, and L. V. Fedina, Soviet Physics JETP **28**, 88 (1969).

[4] D. Schiferl, D. T. Cromer, and J. C. Jamieson, Acta Crystallographica Section B **37**, 807 (1981).

[5] O. Degtyareva, M. I. McMahon, and R. J. Nelmes, High Pressure Research **24**, 319 (2004).

[6] M. I. McMahon, O. Degtyareva, and R. J. Nelmes, Physical Review Letters **85**, 4896 (2000).

[7] O. Degtyareva, M. I. McMahon, and R. J. Nelmes, Physical Review B **70**, 184119 (2004).

[8] Incommensurate composite structures comprise two or more interpenetrating lattice-periodic subsystems, that are mutually incommensurate. Incommensurately modulated structures are those in which atoms are displaced relative to their average lattice-periodic positions by a modulation whose wavelength is incommensurate with the average periodic lattice. The subsystems of an incommensurate composite structure may themselves be modulated as a result of the interactions between them.

[9] K. Aoki, S. Fujiwara, and M. Kusakabe, Solid State Communications **45**, 161 (1983).

[10] R. J. Nelmes, D. R. Allan, M. I. McMahon, and S. A. Belmonte, Physical Review Letters **83**, 4081 (1999).

[11] M. I. McMahon and R. J. Nelmes, Chem. Soc. Rev. **35**, 943 (2006).

[12] M. I. McMahon, O. Degtyareva, R. J. Nelmes, S. van Smaalen, and L. Palatinus, Physical Review B **75**, 184114 (2007).

[13] U. Schwarz, L. Akselrud, H. Rosner, A. Ormeci, Y. Grin, and M. Hanfland, Physical Review B **67**, 214101 (2003).

[14] M. I. McMahon, T. Bovornratanaraks, D. R. Allan, S. A. Belmonte, and R. J. Nelmes, Physical Review B **61**, 3135 (2000).

[15] M. I. McMahon and R. J. Nelmes, Physical Review Letters **93**, 055501 (2004).

[16] S. Falconi, M. I. McMahon, L. F. Lundegaard, C. Hejny, R. J. Nelmes, and M. Hanfland, Physical Review B **73**, 214102 (2006).

[17] E. E. McBride, K. A. Munro, G. W. Stinton, R. J. Husband, R. Briggs, H. P. Liermann, and M. I. McMahon, Physical Review B **91**, 144111 (2015).

[18] R. Briggs, M. G. Gorman, A. L. Coleman, R. S. McWilliams, E. E. McBride, D. McGonegle, J. S. Wark, L. Peacock, S. Rothman, S. G. Macleod, C. A. Bolme, A. E. Gleason, G. W. Collins, J. H. Eggert, D. E. Fratanduono, R. F. Smith, E. Galtier, E. Granados, H. J. Lee, B. Nagler, I. Nam, Z. Xing, and M. I. McMahon, Physical Review Letters **118**, 025501 (2017).

[19] W. Klement, A. Jayaraman, and G. C. Kennedy, Physical Review **131**, 632 (1963).

[20] Z. Jenei, H. Cynn, K. Visbeck, and W. J. Evans, Review of Scientific Instruments **84**, 095114 (2013).

[21] G. W. Stinton, S. G. MacLeod, H. Cynn, D. Errandonea, W. J. Evans, J. E. Proctor, Y. Meng, and M. I. McMahon, Physical Review B **90**, 134105 (2014).

[22] T. S. Sokolova, P. I. Dorogokupets, A. M. Dymshits, B. S. Danilov, and K. D. Litasov, Computers and Geosciences **94**, 162 (2016).

[23] A. P. Hammersley, S. O. Svensson, M. Hanfland, A. N. Fitch, and D. Häusermann, International Journal of High Pressure Research **14**, 235 (2006).

[24] V. Petricek, M. Dusek, and L. Palatinus, Zeitschrift für Kristallographie **229**, 345 (2014).

[25] S. Merkel and N. Hilairet, Journal of Applied Crystallography **48**, 1307 (2015).

[26] H. Iwasaki and T. Kikegawa, Physica **139 & 140B**, 259 (1986).

[27] L. F. Lundegaard, E. Gregoryanz, M. I. McMahon, C. Guillaume, I. Loa, and R. J. Nelmes, Physical Review B **79**, 064105 (2009).

[28] R. Spal, C. E. Chen, T. Egami, P. J. Nigrey, and A. J. Heeger, Physical Review B **21**, 3110 (1980).

[29] L. G. Khvostantsev and V. A. Sidorov, Physica Status Solidi (a) **82**, 389 (1984).

[30] A. Arakcheeva, M. Bykov, E. Bykova, L. Dubrovinsky, P. Pattison, V. Dmitriev, and G. Chapuis, IUCrJ **4**, 152 (2017).

[31] S. van Smaalen, *Incommensurate Crystallography*, International Union of Crystallography Monographs on Crystallography (Oxford University Press, 2007).

[32] P. W. Bridgman, Proceedings of the American Academy of Arts and Sciences **74**, 399 (1941).

[33] S. S. Kabalkina and T. N. Kolobyanina, Soviet Physics JETP **31**, 259 (1970).